

# Properties of Buried SiC Layers Produced by Carbon Ion Implantation in (100) Bulk Silicon and Silicon-on-Sapphire

I. GOLECKI\*§

Consultant  
2222 Los Feliz Drive, #214  
Thousand Oaks, CA 91362

L. KROKO

2822-D Walnut Avenue  
Tustin, CA 92680

H. L. GLASS

Rockwell International Corporation  
Science Center  
3370 Miraloma Avenue  
Anaheim, CA 92803

Buried layers of SiC were formed in (100) single-crystal bulk silicon and silicon-on-sapphire by ion implantation of 125–180 keV,  $(0.56-1.00) \times 10^{18}$  C/cm<sup>2</sup> at 30–40  $\mu$ A/cm<sup>2</sup> into samples held at 450–650° C. The as-implanted and 950° C annealed samples were characterized by differential infra-red absorbance and reflectance, Rutherford backscattering and channeling spectrometry, x-ray diffraction, four-point probe measurements, Dektak profilometry, I-V measurements, spreading resistance measurements and secondary ion mass spectrometry.

**Key words:** SiC, carbon ion implantation, Si, Si-on-sapphire.

## INTRODUCTION

The synthesis of chemical compounds and other modifications of materials by very-high-dose ion implantation are receiving increased attention for applications in electronics, metallurgy and other areas. In particular, the formation of buried, continuous layers of insulators in Si has great significance in the semiconductor field, for achieving new silicon-on-insulator (SOI) technologies. Most of the latter studies have concentrated on SiO<sub>2</sub> and, to a lesser extent, Si<sub>3</sub>N<sub>4</sub>, formed by O and N implantation, respectively.<sup>1</sup> While these compounds are excellent electrical insulators, their mechanical and thermal properties are quite different from those of Si. By comparison,  $\beta$ -SiC, a semiconductor with the cubic zincblende structure and a bandgap of 2.3 eV, which can be obtained with a resistivity greater than  $10^6 \Omega$  cm,<sup>2</sup> is better matched to Si. The atomic densities of single-crystalline Si, single-crystalline  $\beta$ -SiC, amorphous SiO<sub>2</sub> and polycrystalline Si<sub>3</sub>N<sub>4</sub> are 4.99, 4.83, 2.27 and 1.48 ( $10^{22}$  molecules/cm<sup>3</sup>), the corresponding average thermal expansion coefficients between 25 and 1000° C<sup>3</sup> are 3.8, 4.8, 0.46 and 3.3 ( $10^{-6}/^\circ$ C) and the thermal conductivities at room

temperature (RT) are 1.5, 0.4, 0.014 and 0.09 (W/cmK). In addition, cubic  $\beta$ -SiC has been grown epitaxially on Si, starting in the mid-1960's, by chemical vapor deposition<sup>4</sup> and on Si-on-sapphire (SOS) by chemical conversion,<sup>5</sup> in spite of the 20% lattice mismatch:  $a(\beta\text{-SiC}) = 4.3596 \text{ \AA}$ ,  $a(\text{Si}) = 5.4301 \text{ \AA}$  at RT. The orientation relationships between the  $\beta$ -SiC films and the (100) and (111) Si substrates are parallel both in the plane and normal to it.<sup>6</sup> The formation of SiC by ion implantation of C into Si was first reported in Ref. 7 and single-crystalline SiC was reportedly obtained by shallow, 40 keV C implants at  $>10^{17}$  C/cm<sup>2</sup> and  $\approx 700^\circ$  C.<sup>8</sup> This subject was since investigated by a number of other groups, but the most recent and systematic study was reported in Ref. 9. To our knowledge, there has been no report of the formation of SiC by C implantation into SOS films, except our own previous brief conference report.<sup>10</sup> Implantations of O and N into SOS have, however, been investigated.<sup>11</sup>

In the present study, we demonstrate the formation of buried layers of highly oriented SiC by C implantation into bulk Si and SOS. Our aim is to investigate SiC so formed both as an insulator and a semiconductor.

## EXPERIMENTAL CONDITIONS

The 2 inch diameter, commercially available, (100) *n*-type Si substrates used had resistivities of 10  $\Omega$  cm (Czochralski) or 30  $\Omega$  cm (float zone), and the 2 inch diameter, 0.65–0.85  $\mu$ m thick, commercial (100)

\*Work done while affiliated with Rockwell International Corporation, Microelectronics Research & Development Center, 3370 Miraloma Avenue, Anaheim, CA 92803 and a Visiting Associate at the California Institute of Technology, Department of Applied Physics, Mail Code 116-81, Pasadena, CA 91125.

§Present affiliation: Allied Corporation, Corporate Technology, P.O. Box 1021R, Morristown, NJ 07960.

(Received March 10, 1987)

Si films on  $\text{Al}_2\text{O}_3$  were undoped ( $\rho \geq 10^3 \Omega \text{ cm}$ ). The C implantations were performed in the second author's laboratory, with a Varian Extrion 200-A2F ion implanter. In a first set of experiments, Si and SOS wafers were implanted with 180 keV,  $1 \times 10^{18} \text{ C/cm}^2$  at a dose rate of  $\approx 40 \mu\text{A/cm}^2$  over an area of  $\approx 3 \times 3 \text{ cm}^2$ ; the carbon beam was incident at  $0^\circ$ , i.e. normal to the surface. These wafers were not intentionally cooled or heated, and their surfaces reached temperatures of  $450\text{--}550^\circ \text{ C}$ , due to beam heating. In additional runs, Si and SOS wafers were first heated to  $\approx 450^\circ \text{ C}$  and then exposed to the C beam. These wafers were implanted with 150 keV,  $8.85 \times 10^{17} \text{ C/cm}^2$  (Si) or 125 keV,  $(5.62 \text{ or } 7.50) \times 10^{17} \text{ C/cm}^2$  (SOS), at dose rates of  $\approx 30 \mu\text{A/cm}^2$ . The actual surface temperatures of these samples was estimated to be  $\approx 650^\circ \text{ C}$  during the implants. The above doses were chosen to bracket the stoichiometric composition of SiC.

The samples were characterized in the as-implanted state and following 30–180 min. thermal annealing at  $950^\circ \text{ C}$  in flowing  $\text{N}_2$  by the following techniques: differential infra-red (IR) absorbance (Si) and reflectance (SOS), using a Digilab QS 100 Fourier transform IR spectrometer; Rutherford backscattering (RBS) and channeling spectrometry, using 1.6–2.3 MeV  $^4\text{He}^+$  ions; x-ray diffraction (XRD); high-sensitivity four-point probe measurements, using a Four Dimensions 101 instrument; Dektak profilometry; I-V measurements on mesa structures; spreading resistance measurements; and for one sample, secondary ion mass spectrometry (SIMS). Most of the characterization studies, except by the last three techniques, were performed by the first and third authors.

## RESULTS AND DISCUSSION

### General Remarks

Most of the detailed results presented here concern the intentionally heated set of samples, implanted at  $\approx 650^\circ \text{ C}$ , for which no sputtering or surface swelling was detected. The Si and SOS samples heated only by the C beam, on the other hand, were found to have lost  $\approx 1200 \text{ \AA}$  and  $\approx 2000 \text{ \AA}$  of Si, respectively, equivalent to dose-averaged sputtering coefficients of 0.6 (Si) and 1.0 (SOS). We conjecture that in these sputtered samples, an amorphous Si layer was initially formed at the surface, and this amorphous layer had a much larger sputtering coefficient than single-crystalline Si. In the former samples, no amorphous layer was formed at the surface, due to the dynamic annealing of defects and to the ion-beam-induced epitaxial growth occurring above  $\approx 200^\circ \text{ C}$  in Si.<sup>12</sup> In principle, the displacement damage, which in Si is associated with the nuclear elastic collisions, should be reduced for a well-collimated C beam, if it is aligned with a major crystallographic axis. The half-width of the channeling dip for 125–180 keV C  $\rightarrow$  defect-free [100] Si at RT is  $\psi_{1/2} = 1.85\text{--}1.7^\circ$ .<sup>13</sup> However, in the present

case, the reduction in displacement damage due to channeling was probably minor, because of the non-parallel scanning of the C beam and since the energy loss of C at the Si surface is more than 90% electronic.<sup>14</sup> The C-implanted region in the intentionally heated samples was not visible in bulk Si, while it had a light-brown color in the yellow-colored SOS films (even after  $950^\circ \text{ C}$  annealing). Following a brief dip in 10% HF, both C-implanted and unimplanted regions were hydrophobic.

### Infra-Red Measurements

Representative IR spectra are shown in Fig. 1 for bulk Si and in Fig. 2 for SOS; the corresponding parameters are given in Table I. In each case, the reference spectrum for the unimplanted region of each sample has been subtracted electronically, and for the reflectance case, the background spectrum was measured with a high-purity, float-zone Si wafer. Thus, these IR data represent essentially the net effect of the implanted C. All as-implanted samples exhibit one major peak, located at  $790\text{--}793 \text{ cm}^{-1}$  in Si and  $810\text{--}824 \text{ cm}^{-1}$  in SOS. The position of the peak in bulk Si is identical to that reported for SiC.<sup>15</sup> The shift to higher frequencies in the SOS films may be related to the  $\approx -0.4\%$  compressive strain in such films.<sup>16</sup> A 30 min.,  $950^\circ \text{ C}$  thermal annealing results in all the samples in a slight upward shift of  $3\text{--}8 \text{ cm}^{-1}$  in the peak frequency and a reduction of the full-width-at-half-maximum (FWHM) by  $3\text{--}8 \text{ cm}^{-1}$ . The peak areas increase significantly in bulk Si (by 32–50%) but only slightly in SOS (by 5–10%) following the  $950^\circ \text{ C}$  annealing. The increase in peak area signifies an increase in the number of Si-C

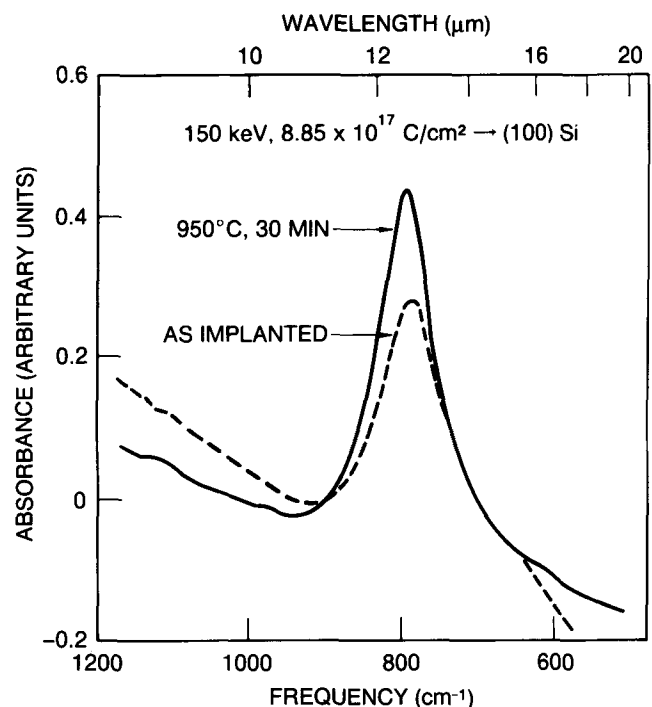


Fig. 1 — Net infra-red absorbance spectra of C-implanted (100) bulk Si.

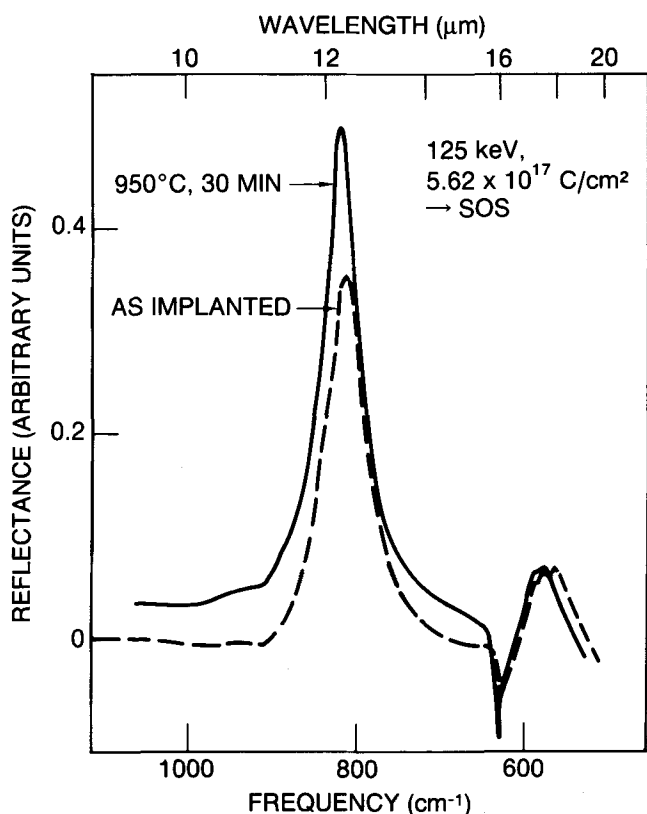


Fig. 2 — Net infra-red reflectance spectra of C-implanted, 0.8  $\mu\text{m}$  thick (100) Si-on-sapphire (from Ref. 10).

bonds. The peak widths in SOS are  $\approx 60\%$  of the values in bulk Si. One bulk Si sample (180 keV,  $1 \times 10^{18}$  C/cm<sup>2</sup>, sputtered) was annealed for an additional 2.5 h at 950°C; the IR spectrum did not change further. A minor peak at  $\approx 600$  cm<sup>-1</sup> was observed in the C-implanted regions of the SOS samples; the area of this peak, which may be due to substitutional C in Si, was  $\approx 4\%$  of the area of the major peak.

#### Rutherford Backscattering/Channeling and SIMS Measurements

RBS/channeling spectra of the Si and SOS samples previously characterized by IR spectroscopy are shown in Figs. 3–4 and the pertinent parameters are given in Table I. These data were measured on the 1 MV Tandem accelerator at the California Institute of Technology. They show that the as-implanted samples consist of a top single-crystalline Si region ( $\approx 800$  Å in Fig. 3a), a transition zone ( $\approx 2400$  Å thick) in which both the defect and carbon concentrations increase monotonically with depth, a SiC<sub>x</sub> region ( $\approx 1600$  Å thick) with  $0.5 \leq x \leq 1.3$ , where the C concentration peaks, a deeper transition zone, where the defect and carbon concentrations decrease monotonically ( $\approx 1200$  Å thick), and finally single-crystal Si. The presence of C is seen both as a decrease in the Si signal (in both random and aligned spectra) and directly as a C signal

**Table I. Results of 1.6 MeV <sup>4</sup>He<sup>+</sup> Rutherford backscattering and channeling spectrometry, differential infra-red reflectance (SOS) and absorbance (Si), and x-ray diffraction measurements of C-implanted (100) SOS and bulk Si.  $\chi_o$  = Si surface channeling yield;  $\chi_m$  = Si channeling yield at the peak of the C distribution; R = depth of C peak;  $x_m$  = maximum C concentration in SiC<sub>x</sub>;  $\omega_o$  = IR peak position;  $\Delta\omega$  = FWHM of IR peak; A = IR peak area = net intensity  $\times$  FWHM (arbitrary units, a.u.);  $\delta\omega$  = FWHM of x-ray peak; S = x-ray peak area = net intensity  $\times$  FWHM (a.u.). The XRD data for the two SOS samples implanted at 125 keV were obtained under the same conditions, but those for the other samples were not; thus the latter peak areas cannot be directly compared. The 180 keV implanted Si sample lost  $\approx 1200$  Å by sputtering during the C implant; the value of R for this sample is as measured, i.e. uncorrected for the sputtering loss. The RBS/channeling values for this sample were obtained with a 2.0 MeV <sup>4</sup>He<sup>+</sup> beam. The channeling yields in these unimplanted SOS films were  $\chi_o = 0.054 - 0.12$  and  $\chi_m = 0.20 - 0.32$ , depending on the sample and the position within the wafer; in the unimplanted bulk Si,  $\chi_o = 0.028$  and  $\chi_m$  (4120 Å) = 0.050.**

Characterization Technique		RBS/Channeling				Infra-Red			X-Ray Diffraction (200) $\beta$ -SiC (400)			
Sample and Processing		$\chi_o$	$\chi_m$	R(Å)	$x_m$	$\omega_o$ (cm <sup>-1</sup> )	$\Delta\omega$	A	$\delta\omega$ (°)	S	$\delta\omega$ (°)	S
125 keV $5.62 \times 10^{17}$ C/cm <sup>2</sup> → 0.8 $\mu\text{m}$ SOS	As-implanted	0.32	0.89	3320	0.84	810	56	20				
	Annealed 950°C, 30 min	0.17	0.85		0.77	818	50	22	1.8	320	2.4	96
125 keV $7.50 \times 10^{17}$ C/cm <sup>2</sup> → 0.65 $\mu\text{m}$ SOS	As-implanted	0.54	0.85	3400	0.98	824	56	36				
	Annealed 950°C, 30 min	0.36	0.87		1.06	830	48	38	1.4	500	2.6	170
150 keV $8.85 \times 10^{17}$ C/cm <sup>2</sup> → (100) Si	As-implanted	0.12	0.84	4120	1.29	790	82	24	1.3	1210	2.7	330
	Annealed 950°C, 30 min	0.09	0.88		1.38	795	79	36	1.4	2670	2.5	1260
180 keV $1.00 \times 10^{18}$ C/cm <sup>2</sup> → (100) Si	As-implanted	0.51	0.97	3500	1.56	793	90	31				
	Annealed 950°C, 30 min	0.30	0.92		1.64	796	83	41	1.0	200	2.3	115

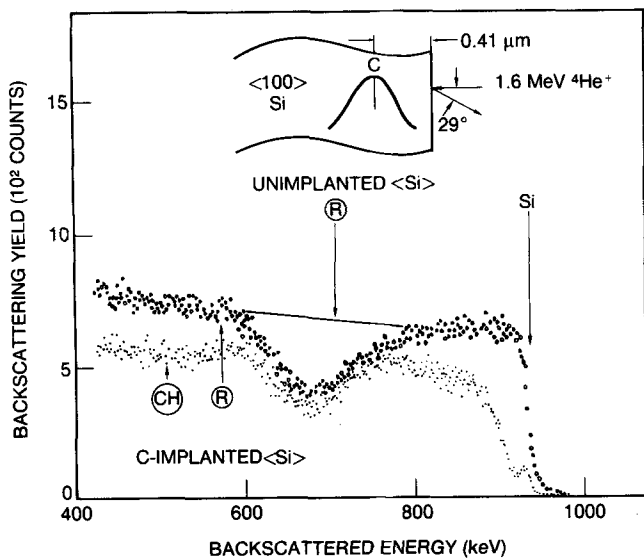


Fig. 3a — Rutherford backscattering and axial channeling spectra of bulk (100) Si implanted with 150 keV,  $8.85 \times 10^{17}$  C/cm<sup>2</sup> at  $\approx 650^\circ$  C (dotted curves). CH = channeled, R = random. The random spectrum of an unimplanted region of the same sample is also shown. The signal from the C atoms, appearing at lower energies, is not shown here. See Table I for numerical values.

appearing at lower energies (Fig. 4a). The thicknesses of the various zones and their crystalline quality, as measured by the channeling yield, vary with implanted dose and with the initial quality of the substrate; the unimplanted SOS films, for example, already have a high concentration of stacking faults, microtwins and dislocations, increasing monotonically from the Si surface towards the Si/Al<sub>2</sub>O<sub>3</sub> interface.<sup>16</sup> However, in the as-implanted bulk Si sample (Fig. 3a),  $\chi_0 = 0.12$ , which is a lower value, indicating a correspondingly better surface crystalline quality, than in most published studies of high-dose O or N-implanted Si, except for a very recent study,<sup>17</sup> where the Si wafers were heated resistively

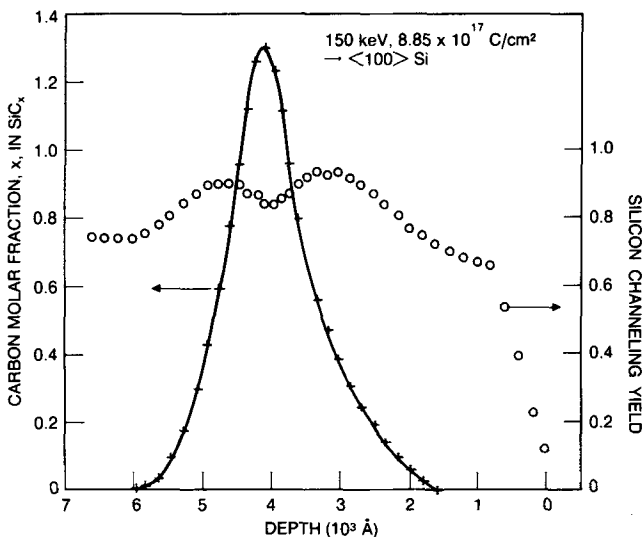


Fig. 3b. — Carbon concentration (crosses and solid curve) and Si channeling yield (circles) in C-implanted bulk Si, calculated from the RBS data of Fig. 3a.

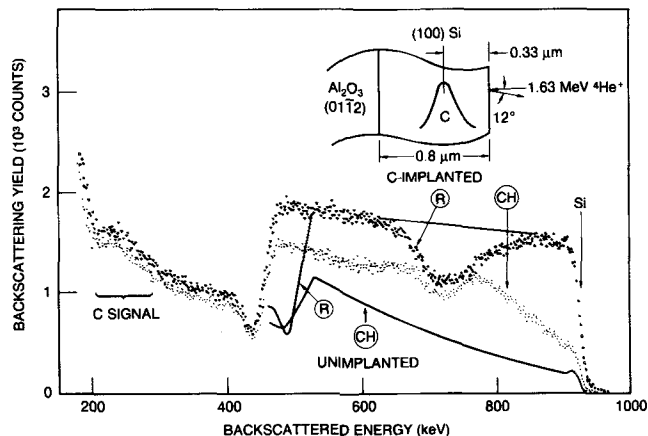


Fig. 4a — Rutherford backscattering and axial channeling spectra of (100) Si/(0112) Al<sub>2</sub>O<sub>3</sub> implanted with 125 keV,  $5.62 \times 10^{17}$  C/cm<sup>2</sup> at  $\approx 650^\circ$  C (dotted curves) and of an unimplanted region of the same sample (solid curves). CH = channeled, R = random. The position of the Si/Al<sub>2</sub>O<sub>3</sub> interface appears at a lower energy in the C-implanted region due to the higher stopping power of this layer (from Ref. 10).

to  $500^\circ$  C during the  $35 \mu\text{A}/\text{cm}^2$ , 180 keV,  $1.9 \times 10^{18}$  O/cm<sup>2</sup> implantation. The Si channeling yield in the SiC<sub>x</sub> region is less than unity in all the samples, and in fact exhibits a relative minimum at the depth corresponding to the peak of the C distribution. The implication of a channeling effect in the SiC<sub>x</sub> region is that this material is at least (100) preferentially oriented polycrystalline, and could even be single-crystalline (although highly defective). This conclusion is supported by the x-ray diffraction data, described below. The  $950^\circ$  C, 30 min. annealing resulted in a large decrease in the channeling yield in the top Si region, signifying the annealing of extended defects there, with a smaller decrease as the C concentration increased with depth. This improvement in crystalline quality was especially ap-

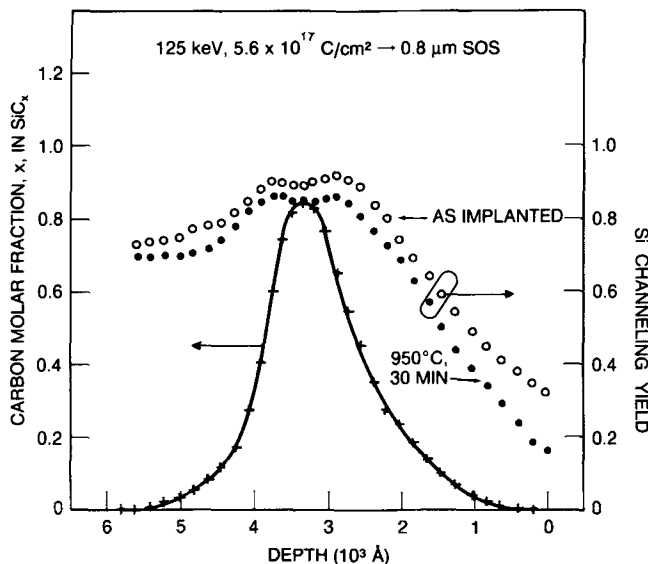


Fig. 4b — Carbon concentration (crosses and solid curve) and Si channeling yield (circles) in C-implanted SOS, calculated from the RBS data of Fig. 4a.

parent in the SOS samples and the sputtered bulk Si sample, where the as-implanted channeling yields were high. The annealing had little effect on the carbon distribution. In order to calculate the carbon profiles quantitatively (e.g. Figs. 3b and 4b), we used the Si signals from the random spectra of C-implanted and unimplanted regions of the various samples. We assumed that C was the only other element present, and that Bragg's rule for calculating the energy loss of the  $^4\text{He}^+$  ions (from Ref. 18) was valid. A numerical iterative procedure was used on a programmable pocket computer. The intrinsic depth scale of RBS, in units of molecules/cm<sup>2</sup>, was converted to Å by assuming a weighted average of the bulk densities of Si and SiC for  $x \cong 1$ , and the density of SiC for  $x < 1$ . The peaks of the C distributions for the 125 and 150 keV implants are  $\approx 30\%$  deeper than predicted in Ref. 14 for C  $\rightarrow$  Si or C  $\rightarrow$  SiC (the predicted C ranges in Si and SiC are the same within 1.5%). The experimental FWHM values are close to the predicted ones for 125 keV C  $\rightarrow$  Si, 15% lower for 150 keV C  $\rightarrow$  Si, and 30% lower for 180 keV C  $\rightarrow$  Si (sputtered sample). In these experimental FWHM, we have already subtracted in quadrature the system resolution, including straggling of the  $^4\text{He}^+$  beam. The measured C profiles could not be fitted by Gaussians, because of the long tails, especially towards the surface. The total carbon dose, obtained from a quantitative measurement of the area under the C distribution, was within 5–20% of the nominally implanted dose, depending on the sample, which is within the combined accuracy of the measurements and calculations. It is not surprising that the peak positions and shapes of these C concentration profiles are different from the values predicted for much lower dose (<1% at.) implants, since the present cases involve ion beam mixing, radiation-enhanced diffusion and sputtering effects, in a matrix of continuously changing composition.

A SIMS depth profile of the  $^{12}\text{C}^-$  ions in the sputtered bulk Si sample was measured using a Cameca IMS-3f spectrometer, with a Cs primary beam. The shape of the C depth distribution was similar to that obtained from RBS. A quantitative comparison would require knowledge of the yield of  $^{12}\text{C}^-$  ions as a function of  $x$  in  $\text{SiC}_x$ . The yield of matrix  $^{29}\text{Si}^-$  ions showed an inverse relation to the  $^{12}\text{C}^-$  yield, decreasing by a factor of 2.1 at the peak of the C distribution.

### X-Ray Diffraction Measurements

The x-ray diffraction scans (Fig. 5 and Table I), performed on a conventional powder diffractometer, using  $\text{CuK}_\alpha$  radiation and a curved graphite monochromator crystal in the diffracted beam, showed only two peaks not due to Si or  $\text{Al}_2\text{O}_3$ . These two peaks could be indexed as corresponding to either the (200) and (400) planes of cubic  $\beta$ -SiC or the (10·4) and (20·8) planes of hexagonal SiC (or possibly a mixture of the two structures). However, based on the known properties of bulk and heteroepitaxial SiC,

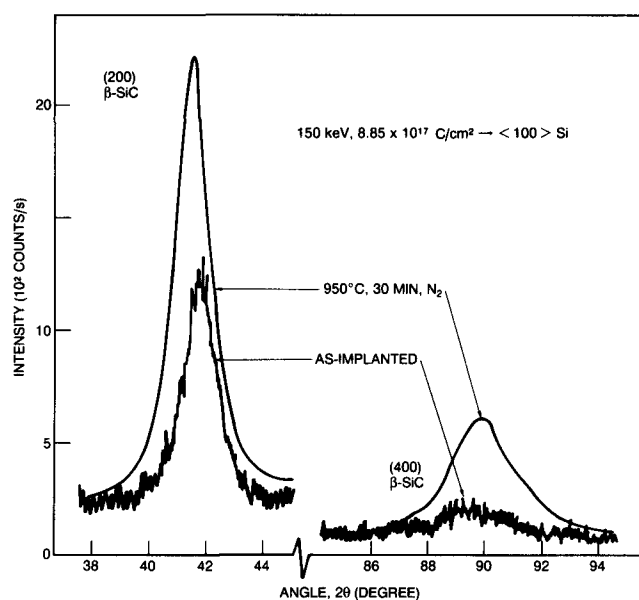


Fig. 5 — Single-crystal x-ray diffraction scans of C-implanted (100) Si, showing only the two peaks not seen in the unimplanted regions of the samples (from Ref. 10).

we will use for the present discussion the cubic assignment. These XRD results thus support the IR data in identifying the chemical SiC in the implanted samples, and the ion channeling data in concluding that the SiC layer is either (100) preferentially oriented polycrystalline or (defective) (100) single-crystalline. Characterization of the buried SiC layers by reflection electron diffraction, transmission electron microscopy and diffraction, or Raman spectroscopy should provide a definitive identification of the microstructure. The 950° C, 30 min. annealing increased the intensities of the (200) and (400) peaks in the bulk Si sample (Fig. 5) by factors of 2 and 4, respectively, while the corresponding FWHM values of 1.3–1.4° and 2.5–2.7° remained unchanged. The increased intensities signify an increase in the number of Si-C bonds, as seen in the IR data following annealing, but could also indicate a reorientation of  $\beta$ -SiC crystallites into the [100] direction and a reduction of local strains. However, the ion channeling data did not indicate an improvement in crystallinity in the SiC layer following annealing. For the two SOS samples implanted at 125 KeV with 7.5 or 5.62 ( $10^{17}$  C/cm<sup>2</sup>), a factor of 1.33 in dose, the ratio of the areas of the (200) peaks was 1.5 and that of the (400) peaks was 1.8. By comparison, the ratio of the IR reflectance peak areas was 1.7, and that of the maxima in C concentrations (from RBS),  $x_m$  in  $\text{SiC}_x$ , was 0.98/0.84 = 1.17.

### Electrical Measurements

Spreading resistance profiles in the bulk Si samples, lapped at 0.6° (Fig. 6), showed a well-defined  $n$ -type region, corresponding in thickness and depth to the  $\text{SiC}_x$  region seen in the RBS spectra, and to a layer of different visual contrast seen in these

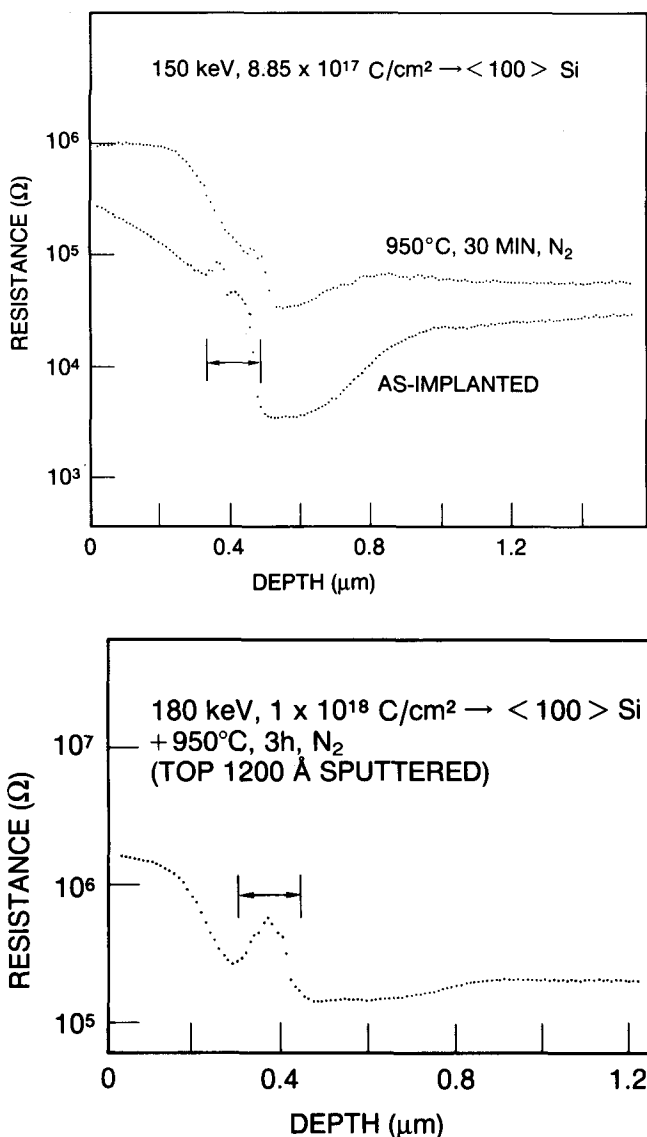


Fig. 6a and 6b — Spreading resistance profiles in C-implanted bulk Si: (a) Czochralski wafer,  $10 \Omega \text{ cm}$ , *n*-type (b) float-zone wafer,  $30 \Omega \text{ cm}$ , *n*-type. The SiC<sub>x</sub> region is marked  $\leftrightarrow$ . Probe load = 10 g, probe separation =  $100 \mu\text{m}$ , probe step =  $1 \mu\text{m}$ , bevel angle =  $0.6^\circ$ .

lapped samples. The average resistivity of the layer was of the same order as that of the Si substrates, and at most a factor of  $\approx 3$  higher (Fig. 6b). The SiC<sub>x</sub> layers in these bulk Si samples were indeed expected to be doped *n*-type, since the Si host crystals were similarly doped, and because of the similar behavior of common dopants in Si and SiC. An additional feature seen was a deeper and  $\approx 50\%$  wider region below the SiC<sub>x</sub>, which had a lower resistivity than the bulk Si, corresponding to a donor concentration in Si of mid- $10^{16}/\text{cm}^3$ . Following a 30 min.,  $950^\circ \text{C}$  annealing, the resistivity in that region increased to a value close to that of the substrate. Thus, the electrical activity in that deeper region was probably due to decoration of deep damage [12] generated by the hot C implant. I-V characteristics measured on a curve tracer were consistent with the spreading resistance profiles. No spreading resis-

tance measurements were made on the SOS samples and therefore the resistivity of the SiC layers formed in these nominally undoped Si films was not determined.

## SUMMARY

The present results demonstrate the formation of a buried layer of SiC chemical compound in 125–180 KeV,  $(0.56 - 1.0) \times 10^{18} \text{ C/cm}^2$  implanted Si and, for the first time, SOS wafers, held at  $450\text{--}650^\circ \text{C}$  during the ion implantation. The chemical nature of the SiC is brought out by the IR and XRD data. Ion channeling and XRD further show that the SiC layer is either preferentially oriented polycrystalline or possibly even single-crystalline (but defective). RBS and channeling measurements show that a high-defect Si region flanks the SiC layer from the top and bottom, but that the Si surface is a relatively good single crystal. The carbon distribution is skewed towards the surface, and there are no atomically sharp Si/SiC interfaces, but rather regions of graded composition. A 30 min.,  $950^\circ \text{C}$  annealing in N<sub>2</sub> significantly improves the Si surface region and increases the number of Si-C bonds, but does not much change the C concentration-depth profile or the crystalline quality of the SiC layer. Heating the wafers to  $450^\circ \text{C}$  prior to the start of and during ion implantation helps prevent the probable initial formation of an amorphous layer and attendant high sputtering of Si. No swelling or sputtering is detected in such intentionally heated samples, implanted at  $\approx 30 \mu\text{A/cm}^2$ , in contrast to the case of high-dose, hot 0 implants.<sup>19</sup> The lack of swelling is due to the good match in atomic density (only 3% difference) between Si and SiC. The SiC layer formed under the present conditions in the *n*-type bulk Si samples is also doped *n*-type, as expected, and thus may have interesting applications as a high-temperature semiconductor. The resistivity of the SiC layers formed in the nominally undoped SOS films was not measured. These and other analytical measurements, as well as additional implantation studies (e.g. into high-resistivity bulk Si) and higher temperature annealing<sup>20</sup> are needed in order to determine the requirements for obtaining an insulating SiC layer by ion implantation.

## ACKNOWLEDGMENTS

One SOS sample (implanted with 180 keV,  $1 \times 10^{18} \text{ C/cm}^2$ ) was measured by RBS/channeling by M. Strathman at Evans & Associates (San Mateo, CA). The spreading resistance measurements were provided by P. Zapella, Aerojet ElectroSystems (Azusa, CA). The SIMS analysis was provided by W. M. Lau, Surface Science Laboratory, University of Western Ontario, Canada.

## REFERENCES

1. For a recent compilation of studies, see Mat. Res. Soc. Symp. Proc. Vol. 53 (1986).

2. Silicon Carbide—1968, *Mater. Res. Bull.* 4, S369 (1969).
3. Y. S. Touloukian, *Thermophysical Properties of High-Temperature Solid Materials*, Vols. 4 and 5 (MacMillan Co.: New York, 1967); Y. S. Touloukian, R. K. Kirby, R. E. Taylor and T. Y. R. Lee, *Thermophysical Properties of Matter*, Vol. 13 (IFI/Plenum: New York, 1977).
4. D. M. Jackson, Jr. and R. W. Howard, *Trans. Metall. Soc. AIME* 233, 468 (1965).
5. I. H. Khan and A. J. Learn, *Appl. Phys. Lett.* 15, 410 (1969).
6. S. Nishino, Y. Hazuki, H. Matsunami and T. Tanaka, *J. Electrochem. Soc.* 127, 2674 (1980).
7. J. A. Borders, S. T. Picraux and W. Beezhold, *Appl. Phys. Lett.* 18, 509 (1971).
8. E. K. Baranova, K. D. Demakov, K. V. Starinin, L. N. Strel'tsov and I. B. Khaibullin, *Dokl. Akad. Nauk SSSR* 200, #4, 869 (1971).
9. T. Kimura, S. Kagiya and S. Yugo, *Thin Solid Films* 81, 319 (1981) and 94, 191 (1982); T. Kimura, S. Yugo, S. Kagiya and Y. Machi, *ibid.* 122, 165 (1984).
10. L. Kroko, I. Golecki and H. L. Glass, *Mat. Res. Soc. Symp. Proc.* Vol. 45, 323 (1985).
11. D. M. Jamba, R. G. Wilson, E. Harari and K. G. Aubuchon, *Final Technical Report, Contract #N00014-75-C-0080* (November 1975), sponsored by Office of Naval Research, monitored by Naval Research Laboratory.
12. I. Golecki, G. E. Chapman, S. S. Lau, B. Y. Tsaur and J. W. Mayer, *Phys. Lett. A* 71A, 267 (1979).
13. H. Grahmann, A. Feuerstein and S. Kalbitzer, *Rad. Effects* 29, 117 (1976).
14. J. F. Gibbons, W. S. Johnson and S. W. Mylroie, *Projected Range Statistics* (Dowden, Hutchinson and Ross, Inc.: Stroudsburg, PA, 2nd ed., 1975).
15. W. G. Spitzer, D. A. Kleinman and C. J. Frosch, *Phys. Rev.* 113, 133 (1959).
16. For a review, see I. Golecki, *Mat. Res. Soc. Symp. Proc.* Vol. 33, 3 (1984).
17. O. W. Holland, D. Fathy, T. P. Sjoreen, J. Narayan and K. More, in *Proc. SPIE—The International Society for Optical Engineering*, Vol. 530, 255 (1985).
18. J. F. Ziegler, *The Stopping and Range of Ions in Matter*, Vol. 4 (Pergamon: New York, 1977).
19. S. R. Wilson and D. Fathy, *J. Electron. Mater.* 13, 127 (1984).
20. G. K. Celler, P. L. F. Hemment, and K. W. West and J. M. Gibson, *Mat. Res. Soc. Symp. Proc.* Vol. 53, 227 (1986).